frontiers in Nuclear Engineering

TYPE Original Research
PUBLISHED 09 March 2026
DOI 10.3389/fnuen.2026.1787346

OPEN ACCESS

EDITED BY
Tao Wu,
Huzhou University, China

REVIEWED BY
Simon Norris,
Independent Researcher, London, United Kingdom
Chun-Ping Jen,
National Chung Cheng University, Taiwan

*CORRESPONDENCE
Stefan Finsterle,
stefan@finsterle-geoconsulting.com

RECEIVED 14 January 2026
REVISED 05 February 2026
ACCEPTED 06 February 2026
PUBLISHED 09 March 2026

CITATION
Finsterle S, Hannon MJ Jr. and Sloane J (2026) Identification of safety-relevant radionuclides for performance assessment modeling.
Front. Nucl. Eng. 5:1787346.
doi: 10.3389/fnuen.2026.1787346

Identification of safety-relevant radionuclides for performance assessment modeling

Stefan Finsterle[1]*, Michael J. Hannon Jr.[2] and Jesse Sloane[3]

[1]Finsterle GeoConsulting, LLC, Kensington, CA, United States, [2]Hannon Clean Energy, LLC, Bloomington, IN, United States, [3]Deep Isolation Nuclear, Berkeley, CA, United States

We propose, apply, and verify a screening approach for the selection of safety-relevant radionuclides that should be tracked in models assessing the performance of geologic repositories for the disposal of spent nuclear fuel and high-level radioactive wastes. Starting with a comprehensive list of radionuclides present in the waste form, a multi-step down-selection process evaluates each isotope's potential relative contribution to the total peak exposure dose, which is a surrogate metric for overall repository safety. In the first screening step, only basic, readily available characteristics of a radionuclide are needed, such as its inventory, half-life, specific activity, and dose coefficient. In the second step, the radionuclide's transport time from the repository to the accessible environment is estimated based on factors affecting its mobility and retardation. By adjusting the screening threshold, the number of radionuclides considered potentially safety-relevant can be changed, thus yielding a larger or smaller (more or less conservative) set of radioisotopes being tracked in the performance assessment model, as warranted by the stage of repository development. We exercise the proposed screening approach for a particular waste form—spent nuclear fuel assemblies—and two disposal pathways—deep horizontal and vertical borehole repositories. An integrated performance assessment model is then used to simulate the migration of a considerably larger set of radionuclides from the disposal canisters to the land surface. The acceptably small difference in peak dose calculated with the comprehensive and reduced set of radionuclides indicates the appropriateness of the proposed screening approach.

KEYWORDS
borehole repository, iTOUGH2, peak exposure dose, performance assessment, radioactive waste disposal, radionuclide screening model, validation

1 Introduction

Spent nuclear fuel and high-level radioactive waste from used fuel reprocessing, power plant decommissioning, coolant waste, as well as research, or medical and industrial applications contain a wide range of radioisotopes. They include fission products, actinides, and other isotopes mainly generated by neutron absorption. The radionuclides in the waste inventory have a very large range of half-lives and specific activities, and their radiological impact on humans varies depending on their decay type (alpha, beta, or gamma decay), the exposure pathway, and biological factors, which determine the potential for harm. Depending on their chemical form, radionuclides may be volatile, highly soluble in liquid fluids, or prone to precipitation and adsorption onto solids, making them either highly mobile or strongly retarded as they are being transported through the engineered barrier system and natural environment from the waste form to the accessible environment.

This large variety of radionuclides and their characteristics makes it evident that the health risks posed by radioactive waste strongly depends on its age, location, and the surrounding physical, chemical, and biological conditions, requiring different strategies to condition, handle, and contain the waste, to protect humans, and to reduce the risk and mitigate the consequences of events that lead to the release of radionuclides to the environment. In the specific context of this paper, it is important to note that the list of radionuclides posing the greatest safety concerns changes drastically with time and the particular stage of the back end of the nuclear fuel cycle we are considering. Here, we focus on the final stage, i.e., disposal of the waste in a deep geologic repository.

The basic principle of geologic disposal is to isolate the waste, or to sufficiently delay its release, with the effect that only a fraction of the radionuclides reaches the accessible environment after a very long time relative to the radionuclides' respective half-lives. It is mainly this time component that allows many of the radionuclides initially present in the waste inventory to decay to levels that no longer cause any adverse health effects once they reach the biosphere. A geological repository with its engineered and natural barriers can provide the long-term protection needed to allow for sufficient decay of most radionuclides, which drastically reduces (a) the number of safety-relevant radionuclides, (b) the risk of them being released to the accessible environment, and (c) the concentration and thus consequences of such a release. This is also the reason why a post-closure performance assessment—and the radionuclides involved in such an assessment—is very different from a pre-closure evaluation of accident scenarios.

For the discussion that follows, we focus on the peak exposure dose that an individual member of the public may receive by ingesting contaminated groundwater from a well located immediately above the repository during a performance period of 10 million years. (Note that different definitions or locations of the compliance boundary and additional exposure pathways can be accounted for in the proposed screening approach by choosing the appropriate transport distance and dose conversion factor, respectively.) This measure (a) integrates the performance of the entire repository system, and (b) is likely compared against the key safety standard in a license application for a geologic repository. The regulatory standard is typically defined as a total effective dose equivalent that does not exceed 0.1 mSv in a year, exclusive of the dose contributions from natural background radiation and medical procedures.

The safety case of a geologic repository relies to a large extent on a long-term performance assessment (PA) calculation, which is provided by numerical simulations involving all relevant features, events, and processes (FEPs) occurring in the repository system from the time of repository closure to the end of the performance period. Ideally, all radionuclides initially present in the waste form are examined in a PA calculation. For a variety of reasons, this approach is impractical, unnecessary, or unwarranted. Particularly for a preliminary analysis, whose purpose is to get an initial assessment of the viability of the disposal concept, the calculations are by design simplified and generic, i.e., based on reference conditions and some limiting cases as part of a sensitivity analysis. The results of such an analysis are inevitably only approximate, a fact that can be considered acceptable for the intended use of the model. This needs to be clearly communicated, which includes selecting an approach that does not suggest a level of accuracy in certain input parameters that is inconsistent with the attainable accuracy of the model output. A repository license application will be based on a much more detailed, site-specific PA model, with more radionuclides tracked for a comprehensive evaluation of repository performance.

PA simulations are conceptually and numerically challenging, requiring the formulation and documentation of defensible abstractions, assumptions, and parameter choices. Given that the PA model must capture complex coupled processes occurring in many components of the engineered and natural barrier systems over a range of scales and over a long prediction period, the computational costs for such simulations are considerable. Each radionuclide tracked in the simulation adds a mass balance equation to the set of non-linear partial differential equations that need to be repeatedly solved using Newton-Raphson iterations for each time step. Furthermore, PA models are often run repeatedly within a stochastic framework, where a computational tradeoff must be made between the accuracy of the individual simulation and the number of realizations that can be afforded. For this reason alone, only those radionuclides that are expected to have a noticeable impact on the outcome of the safety calculation should be tracked in the model.

In Section 2.1, we present a methodology that helps identify the potentially safety-relevant radionuclides that should be included in a PA model. The multi-tier selection approach relies on basic characteristics of each radionuclide and some estimates of their transport time through the engineered and natural barrier systems. The approach is flexible in that it can be adjusted to the accuracy warranted by the current stage of repository development, i.e., from initial screening calculations to the evaluation of design alternatives, development of site selection criteria, viability studies, to a comprehensive safety analysis in support of a license application. In Section 2.2, we briefly describe a previously developed, integrated PA model, which will be used to test the appropriateness of the proposed radionuclide screening process. Section 3.1 demonstrates radionuclide selection based on the inventory of one particular waste form—spent nuclear fuel (SNF) assemblies from commercial pressurized water reactors (PWR)—and the disposal in two repository types—a deep horizontal borehole repository and a deep vertical borehole repository (Muller et al., 2019; Finsterle et al., 2020; Finsterle et al., 2021a; Finsterle et al., 2021b)—in the context of analyzing the nominal scenario. Finally, in Section 3.2, a PA calculation is performed involving a larger set of radionuclides to test whether the screening approach indeed identified the most safety-relevant radionuclides without an undue underestimation of the peak exposure dose.

2 Materials and methods

2.1 Approach for selecting safety-relevant radionuclides

In this section, we outline the approach to select the radionuclides that are potentially safety-relevant and should be included in the PA model calculations used for the evaluation of the performance metrics. Note that the term "safety-relevant" refers to the need to track the corresponding radionuclide in a specific PA

model to approximate total dose; it is not a regulatory classification indicating compliance. For the reasons given above, an approach is sought to estimate each radionuclide's *potential* safety-relevance. The evaluation should be based on a small number of factors that are either well known or can be estimated with limited information and effort. Estimating the safety-relevance of a radionuclide based on a small set of factors is clearly insufficient to assess repository performance, and even less so to indicate regulatory compliance. Nevertheless, it is important to make sure that all potentially safety-relevant radionuclides are included in any quantitative evaluation of repository performance, minimizing the risk that omission of a radionuclide does not lead to a significant underestimation of exposure dose, even in the preliminary stages of repository assessment.

The general multi-step approach for the identification of safety-relevant radionuclides includes the following steps:

1. Compile an initial list of potentially safety-relevant radionuclides, typically identical to the list of radioisotopes present in the waste form.
2. Identify likely factors that affect the performance metric of interest (here: peak exposure dose); only factors related to radionuclide-specific properties need to be considered.
3. Combine factors into subsets according to their relevance and ease of calculation (see below).
4. Evaluate all factors of the current subset for each radionuclide of the current list. The multi-tiered process starts with an evaluation of the comprehensive list of radionuclides identified in Step (1) and factors that are easy to evaluate based on readily available data. While subsequent steps only involve the radionuclides that passed the previous screening criterion (see Step (7) below), they involve more complex factors that require the determination of additional parameters.
5. Condense the evaluations in Step (4) into a score that is comparable across all radionuclides.
6. Rank the radionuclides according to their total score and normalize the scores to that of the highest-ranked radionuclide.
7. Define a cut-off value to separate the safety-relevant from the safety-irrelevant radionuclides; this step shortens the list of potentially safety-relevant radionuclides.
8. Repeat Steps (4) to (7) for all subsets defined in Step (3).
9. If considered necessary, the procedure can be repeated with different assumptions about parameters that depend on end-member scenarios to examine the robustness of the selection scheme.

The initial list of potentially safety-relevant radionuclides (see Step (1)) should be comprehensive, e.g., based on the list of radioisotopes present in the waste form, plus potentially significant decay products. The list can also be based on existing catalogs of safety-relevant radionuclides, supplemented by isotopes specific to the given waste form, e.g., those generated by advanced reactors or accumulated during processing or recycling of used nuclear fuel and other highly radioactive wastes.

The identification of quantifiable factors indicative of a radionuclide's safety-relevance (see Step (2)) requires a *general* understanding of the total system behavior and the influence of certain FEPs on the performance metrics along with the FEPs-related, quantifiable model input parameters. Only FEPs that lead to different exposure doses because of the specific properties of a radionuclide need to be considered. Such FEPs are mainly related to the waste form, but also solute transport, geochemistry, biology, and radiology.

The factors can be grouped as follows:

1. Characteristics of the radionuclide: half-life, dose coefficient, and solubility limit.
2. Waste form: the inventory of each radionuclide in the waste form.
3. Conditions of the repository system and their influence on radionuclide transport: parameters affecting retardation (sorption and matrix diffusion).

Ideally, all the factors of all radionuclides initially present in the waste form are exhaustively evaluated to obtain a complete, ranked list of each radionuclide's safety-relevance. However, a more pragmatic approach is chosen here, in which the factors are evaluated sequentially. Intermediate scores are calculated, the radionuclides are ranked, and the list is truncated before the next set of factors is examined.

The first subset consists of factors for which the corresponding model input parameters are either well known, or reasonable values can be obtained with only a few auxiliary assumptions. The first intermediate score is the product of radionuclide-related parameters and requires a preliminary estimate of transport time:

$$S_{1,i} = m_{0,i} \cdot a_i \cdot dcf_i \cdot e^{-\lambda_i \cdot t_t} \tag{1}$$

Here, $m_{0,i}$ (kg) is the initial inventory mass of radionuclide i in the waste form, $\lambda = \ln(2)/t_{1/2}$ (s^{-1}) is the decay constant with $t_{1/2}$ (s) being the half-life, $a = \lambda \cdot N_A/M$ (Bq kg^{-1}) is the specific activity, where M (kg mol^{-1}) is the molecular weight and $N_A = 6.022 \times 10^{23}$ (mol^{-1}) is the Avogadro constant, t_t (s) is an estimate of the time needed for the radionuclide to reach the accessible environment, and dcf_i (Sv Bq^{-1}) is the dose coefficient. This intermediate score states that the exposure dose is approximately proportional to the radionuclide's abundance in the waste, its rate of generating ionizing radiation, how much decays while migrating from the repository to the land surface, and its toxicity to humans.

Setting $m_{0,i}$ as the initial inventory of radionuclide i in the canister may underestimate the actual amount if the radionuclide is the daughter product of another isotope. The total mass of the decay product can be approximately estimated by adding all parent radionuclides within its decay chain and calculating ingrowth over the presumed transport duration. For example, the potentially safety-relevant radionuclide ^{237}Np has an initial mass of 1.24 kg (Carter et al., 2012) per canister, each holding a spent fuel assembly. However, ^{237}Np is continuously generated by the decay of ^{241}Am, which has an initial inventory of 1.25 kg, but a small amount is also generated by the decay of ^{245}Cm, which has an initial inventory of 0.01 kg. To account for ingrowth the mass of each daughter product i is calculated as the sum of its initial mass in the canister, $m_{0,i}$, plus the total amount generated by the decay of its

parent radionuclide $i-1$ by the parent radionuclide's estimated transport time to the biosphere (in this example assumed to be 400,000 years):

$$m'_{0,i} = m_{0,i} + m'_{0,i-1} \cdot \frac{M_i}{M_{i-1}} \cdot \left(1 - e^{-\lambda_{i-1} \cdot t_t}\right) \quad (2)$$

Here, M_i is the molecular weight of radionuclide i. Given the short half-life of ^{245}Cm (compared to the transport time), the entire initial inventory of ^{245}Cm will decay and be added to the mass of ^{241}Am, which in turn will decay completely to ^{237}Np. As a result, the mass of ^{237}Np, accounting for ingrowth, is approximately $m'_{0,Np} = 0.01 + 1.25 + 1.24 = 2.5$ kg. For parent radionuclides that are part of a decay chain and have a half-life that is comparable to the transport time t_t, only a fraction of their mass will decay and be added to that of the daughter product.

In Equations 1, 2, the inventory $m_{0,i}$ depends on the fuel type and some of the reactor's operational parameters (e.g., initial enrichment, burn-up, and waste loading factor) as well as the properties of the waste form, in particular if the waste stream is generated by reprocessing, recycling, or conditioning of used nuclear fuel.

A radionuclide's half-life $t_{1/2}$ (and therefore its decay constant λ and specific activity a) is typically well known and can directly be taken from published tables of radioisotope properties. Dose coefficients dcf depend on the exposure pathway and the details of the biosphere model. The PA model makes use of the IAEA ERB1A reference biosphere model for solid radioactive waste disposal (IAEA, 2003). The relative toxicity of the radionuclides is properly represented by the dose coefficients for ingestion tabulated in ICRP (2012). Note that relatively short-lived daughter products are included in the dose coefficient of the parent radionuclide by assuming they are in secular equilibrium with the parent.[1]

At time t_t when the peak dose in the accessible environment is reached, radioactive decay has reduced the initial mass m_0 to $m_0 \cdot e^{-\lambda \cdot t_t}$. The peak dose time is obviously not known *a priori* but is the result of the simulation with the PA model. Nevertheless, an approximate estimate of that time is sufficient for the purpose of radionuclide screening. Recall that the basic concept of waste disposal in a deep geological repository is primarily to delay the release of radionuclides to the accessible environment, thus allowing decay to exponentially reduce concentrations in the drinking water aquifer. The effectiveness of this reduction relies not only on the radionuclide's half-life, $t_{1/2}$, but also on properties of the repository system, including canister performance, repository depth or—more generally—length of the migration pathway, and transport velocity in the geosphere. The migration time of a radionuclide that is conservatively assumed to be non-sorbing in a porous host rock can be estimated as follows:

$$t_t = t_b + t_{diff} + t_{adv} \quad (3)$$

Here, t_b is the canister breach time, and t_{diff} and t_{adv} are the diffusive and advective transport times, respectively.

Equation 3 assumes that transport through the various repository system components is either diffusion- or advection-dominated, and that the components are aligned in series (rather than in parallel). This is appropriate for most configurations, including a system where radionuclides first migrate by advection or diffusion through the components of the engineered barrier system (EBS), then by diffusion through porous host formations (such as clays) or by advection through a fractured bedrock, then by diffusion through a low-permeability sedimentary overburden, and finally by advection within the aquifer to the drinking water well. This assumption appears to be violated when considering, for example, fast fluid flow directly from the repository to the accessible environment through a reactivated fault or leaking access structure. These configurations could be represented by a flow-in-parallel equation (i.e., using the reciprocal of the sum of the reciprocal resistant terms). However, as demonstrated in Finsterle et al. (2020), Finsterle et al. (2021a), the fraction of radionuclides transported through such fast-flow channels is very small in comparison to the inventory. Because fast-flow pathways reduce migration times, it is likely that a different set of potentially safety-relevant radionuclides needs to be determined using the approach presented here and propagated through a separate PA model that specifically addresses disruptive event scenarios.

A first estimate of t_{diff} can be obtained by calculating the time needed for a conservative tracer to diffuse through the engineered barrier system and/or through the argillaceous host rock. This time can be estimated as:

$$t_{diff} = \frac{L_{diff}^2}{\Sigma} \quad (4)$$

where L_{diff} (m) is the distance the radionuclides travel through a diffusion-dominated material, and Σ (m^2 s^{-1}) is an estimate of the effective diffusion coefficient, which is based on the molecular diffusion coefficient but reduced to account for porosity and tortuosity. The inclusion of temperature effects on diffusion is not warranted for the purpose of radionuclide screening. Equation 4 assumes diffusion through a linear system, which is appropriate if the disposal section is relatively long and the spacing between disposal sections is relatively short compared to the depth of the repository; the assumption yields shorter transport times compared to cylindrical or spherical solutions.

For a fractured host rock, an estimate of the advective transport time through the fracture network can be obtained by making assumptions about hydraulic conductivity K (m s^{-1}), porosity ϕ (–), and the hydraulic head gradient ∇H (m m^{-1}):

$$t_{adv} = \frac{L_{adv} \cdot \phi}{K \cdot \nabla H} \quad (5)$$

Here, L_{adv} (m) is the distance the radionuclides travel within the advection-dominated migration pathway. During the second screening iteration, the estimate of the transport time t_t is refined by accounting for retardation mechanisms (sorption and matrix diffusion).

After the evaluation of $S_{1,i}$ for all radionuclides i of the initial list of potentially safety-relevant radionuclides, the list is ranked. As the first screening criterion, all radionuclides with a normalized score of

1 Contributions of the progeny radionuclides to dose are included in the dose conversion factor of the following parent radionuclides: ^{90}Sr, ^{93}Zr, ^{226}Ra, ^{229}Th, ^{231}Pa, ^{232}Th, ^{237}Np, ^{235}U, ^{238}U, ^{243}Am, and ^{245}Cm.

10.3389/fnuen.2026.1787346

less than a suitable threshold value (e.g., 10^{-6}) of the highest-scoring radionuclide are removed from the list.

In the remaining screening stages, processes and parameters related to retardation and solubility limits are considered. They are more difficult to integrate into the safety-relevance score, as they depend on the details of the repository system and the conditions in the geosphere.

In the second subgroup we consider factors that affect radionuclide transport. Sorption of radionuclides to the solid phase leads to a retardation in solute transport, i.e., delayed arrival of radionuclides in the biosphere and thus reduced concentrations due to additional radioactive decay. A retardation factor R_{Kd} (–) can be defined under the simplifying assumptions of reversibility and instantaneous equilibration as (de Marsily, 1986):

$$R_{Kd} = 1 + \left(\psi \rho_s K_d / \phi\right) \tag{6}$$

Here, ρ_s (kg m^{-3}) is the density of the rock grains, and K_d (m^3 kg^{-1}) is the aqueous phase distribution coefficient. For porous host rocks, all grains are assumed to be in contact with the percolating radionuclide-carrying water (referred to as "bulk reaction"). For sparsely fractured crystalline host rocks, the radionuclides may sorb onto fracture surfaces (referred to as "surface reaction"). However, the retardation capacity of the fractured host rock may be considerably higher if radionuclides diffuse into the essentially stagnant pore water of the rock mass between the fractures (referred to as "matrix diffusion"). Typically, only a fraction of the matrix volume is effectively accessible by matrix diffusion and thus available for sorption. To account for this effect, the utilization factor $\psi = 2\eta/S$ is introduced, with η being the penetration depth and S the fracture spacing. The utilization factor may be very small if the fracture spacing is relatively large, or the penetration depth is short due to reduced diffusivities in the zone near the fracture walls caused by mineralization and other geochemical reactions. The retardation factor for matrix diffusion in fractured rock approaches a value of (Neretnieks, 1980):

$$R_{md} = 1 + \frac{\psi \cdot \phi_m \cdot \left(1 - \phi_f\right)}{\phi_f} \tag{7}$$

where ϕ_m and ϕ_f are the porosities of the rock matrix and fracture, respectively.

For the purposes of radionuclide screening, only an approximate retardation factor due to matrix diffusion is sought. If adsorption on the fracture surfaces or within the rock matrix is included, retardation is further enhanced by the corresponding factor R_{K_d} of Equation 6. The combined effects of diffusion and sorption within the radionuclide penetration zone near the fracture-matrix interface is described in detail in Neretnieks (1980), who also discusses the dependence on fracture and matrix properties as wells as other factors and assumptions.

In addition to their effects on transport time, both sorption and matrix diffusion lead to a flattening of the radionuclide breakthrough curve, thus further reducing peak dose. However, this beneficial effect is not accounted for in these screening calculations.

The second intermediate score, S_2, is identical to S_1 defined in Equation 1, with the exception that the time variable t_t is amended by the radionuclide-specific retardation factors R_{Kd_i} and R_{md_i}:

$$S_{2,i} = m_{0,i} \cdot a_i \cdot dcf_i \cdot e^{-\lambda_i \cdot R_{Kd_i} \cdot R_{md_i} \cdot t_t} \tag{8}$$

The list of potentially safety-relevant radionuclides is now further truncated by normalizing $S_{2,i}$ and applying a threshold value as described above.

Finally, in a third screening iteration, we account for the fact that the maximum concentrations of a radionuclide in pore water may be constrained by its solubility limit. Note that radionuclide concentration can only increase (and potentially reach the solubility limit) if the congruent release rate of radionuclides from the degrading waste form is higher than the rate with which the radionuclides are transported away by advection and diffusion. An upper bound for dose is given by the radionuclide concentration in the liquid phase at the source of contamination at the time they are released. This maximum concentration depends on (a) the inventory, (b) the waste degradation and radionuclide release rates (including a potential "instant release fraction"; *IRF*), (c) the water volume available for dilution and mixing in the immediate vicinity of the release point, (d) the effective diffusion coefficient and advective flow rate carrying away the dissolved radionuclides, and (e) the thermal and geochemical conditions that impact the solubility limit itself. This multitude of factors complicates the inclusion of the solubility limit as a criterion for the selection of safety-relevant radionuclides.

If the solubility limit is not reached, the relative concentrations of dissolved radionuclides is given by their relative amounts in the inventory, which is already accounted for through the m_0 term in Equation 1. This means that accounting for the solubility limit as a screening criterion only helps remove species from the list of safety-relevant radionuclides if their theoretical, inventory-limited concentration greatly exceeds the solubility limit. Both the inventory-limited concentration and geochemical solubility limits have been evaluated by Bates (2015) for granitic bedrock chemistries under the assumption that the entire inventory is instantaneously released (i.e., *IRF* = 100%) into a finite, relatively small volume of pore water. In reality, however, radionuclides are very slowly released from the degrading waste form, and *IRF* values are small for most radionuclides. Furthermore, the volume for dissolution is typically not limited or constant as radionuclides are dispersed by diffusion and advection, reducing the concentration near the source and thus delaying the time until the solubility limit is reached, if at all. Even if the limit were reached (as is expected for some radionuclides such as ^{99}Tc), it would only be a temporary effect, as the concentrations will eventually become lower than the solubility limit by the reduction of the congruent release rate or the depletion of the inventory, both being further affected by radioactive decay. Only if the *IRF* or waste degradation rates were indeed very high may it be advisable to account for imposing a temporary constraint on concentrations and delayed mobilization because of reaching the solubility limit. The (unrealistic) assumption that each radionuclide is released with an *IRF* of 100% could lead to the conclusion that their concentrations should be curtailed to the solubility limit, thus unduly reducing their safety-relevance even for the case where this limit is not reached. Also note that due to potential supersaturation, the kinetic solubility limit may temporarily exceed the equilibrium-based limit, which would lead to a non-conservative underestimation of a radionuclide's mobility.

Nevertheless, as the dissolution and thus mobilization of some radionuclides may be constrained by the solubility limit, this effect could be accounted for by using the ratios of the inventory-limited to the solubility-limited concentrations of Bates (2015) as an additional factor, f_{sol}:

$$f_{sol} = min\left(1, \frac{C_{solubility-limited}}{C_{inventory-limited}}\right) \quad (9)$$

The calculation of the inventory-limited concentration could be amended by accounting for the ratio of the radionuclide release rate from the degrading waste form and the diffusive radionuclide transport rate away from the canister. This may require abstracting results from reactive transport simulations to also account for the changing conditions and feedback mechanisms within the EBS and near field of the repository. If accounting for solubility limit is considered relevant, this effect can be added to a third score:

$$S_{3,i} = S_{2,i} \cdot f_{sol,i} \quad (10)$$

After ranking, normalizing, and applying the cut-off criterion, a final list of potentially safety-relevant radionuclides is obtained. The radionuclides on that list should be included in the PA model.

As stated above, this screening process for identifying safety-relevant radionuclides is based on a highly simplified calculation of the *relative* contributions of individual radionuclides to peak dose. Since some of these factors—specifically the retardation effects due to sorption and matrix diffusion, and the effects from reaching the solubility limit—depend on additional parameters and assumptions that are either not well known or vary considerably over the parameter space and the range of scenarios typically evaluated by a PA model, the robustness of the approach must be tested. This can be done by repeating the screening process with different assumptions about the underlying parameters to see if the final ranking and list of safety-relevant radionuclides changes. The union of the sets of safety-relevant radionuclides obtained with different input factors should then be propagated to the PA analysis. This approach should be used specifically for probabilistic assessments, where the PA model is run for a wide range of uncertain input parameters.

The list can also be compared to results obtained from safety calculations performed with comprehensive performance assessment models that track a larger set of radionuclides. If the results of the screening analysis vary considerably depending on the assumptions, the list of potentially safety-relevant radionuclides should be expanded. This can be achieved by either reducing the cut-off criterion, or by stopping the screening after the first iteration, i.e., without truncating the list based on the evaluation of secondary or tertiary factors, as discussed above.

Conversely, the list may be too long and cannot practically be propagated through the PA model. In this case, the list can be shortened by (a) increasing the cut-off criterion, (b) performing additional iterations with newly evaluated screening factors, or (c) adding a safety factor to the results of the PA model. Note that the magnitude of the safety factor can be based on the chosen cut-off criterion, as it is expected that the relative underestimation of peak-dose contributions of the excluded radionuclides is given by the sum of the scores of the discarded radionuclides, normalized by the sum of the scores of the radionuclides included in the PA calculation.

The threshold value should be chosen predominantly to reflect the purpose of the modeling study to be performed by the PA model. For example, if the PA model is a highly simplified compartment model used to examine the relative performance of generic site conditions or design alternatives, it is likely sufficient to set a comparatively high threshold value (e.g., 0.1), for the sole purpose to make sure the simulation is based on the properties of the most safety-relevant radionuclide. The threshold value should be reduced (thus conservatively including more radionuclides) only (a) if warranted by the amount and quality of the data supporting the PA model, or (b) if specific processes are included in a high-fidelity PA model whose impact on relative dose contribution is not well captured by the few adjustable factors of the screening model.

Finally, we briefly compare our proposed approach with the screening analysis described in Nagra (1994). The main difference is the choice of the cut-off criterion—absolute versus relative—and the location where the metrics are evaluated. In Nagra (1994), exposure dose is estimated at the time of canister failure at the location of the canister; transport through the engineered and geological barriers is neglected. The so-called dose index is calculated, which is defined as the estimated, *absolute* dose value divided by the regulatory limit of 0.1 mSv yr^{-1}. All radionuclides with a dose index higher than a cut-off value of 10^{-3} are considered safety relevant. By contrast, our approach uses the dose ratios as a *relative* selection metric, acknowledging that a simple screening calculation cannot provide an accurate estimate of the *absolute* exposure dose; this will be accomplished by the high-fidelity PA model.

This conceptual difference affects the choice of factors used to select the list of safety-relevant radionuclides. For example, Nagra (1994) uses the waste dissolution rate to calculate the absolute radionuclide concentration in the pore water, which is then directly converted to the absolute exposure dose. While the waste degradation rate indeed impacts the peak dose value (see Finsterle et al. (2025a) for a detailed analysis of the influence of source-term parameters on peak dose), it does not affect a *relative* selection criterion specifically if the assumption of congruent radionuclide release from the degrading waste form holds. But even if this assumption is violated (for example, if a fraction of a radionuclide is instantly released upon canister breach—an effect that is included in the PA model), the impact is limited (Finsterle et al., 2025a) and therefore does not change the screening measure or radionuclide ranking. Similarly, as non-sorbing radionuclides do not undergo significant segregation, the effects of dispersion, dilution, and mixing do not affect the relative selection criterion. Most importantly, our screening approach includes transport through the near field and geosphere. Screening out radionuclides that decay to insignificant levels due to long transport times accounts for the geosphere's barrier function, which is at the core of geologic waste disposal. Nevertheless, our approach can also be used for scenarios in which the geologic barriers are bypassed (e.g., by human intrusion) by setting the transport distance and thus transport time to essentially zero. Note that for their general license application, Nagra changed its screening approach by using, in a first stage, a highly conservative and simplified transport model to select potentially safety-relevant radionuclides (Nagra, 2024). The relatively long list of radionuclides passing the first-stage selection criteria is then considerably reduced using a high-fidelity PA model, before computationally intensive probabilistic calculations are performed.

2.2 Post-closure performance assessment models

The approach described above for estimating the radionuclides' relative safety-relevance is based on just a few properties of the radionuclides combined with highly simplified assumptions about their release from the canisters and transport through the geosphere. To test whether the proposed screening process indeed only excludes radionuclides whose contributions to the total exposure dose are acceptably small, a larger set of radionuclides is simulated using a high-fidelity PA model. The total exposure dose calculated with the reduced set of radionuclides can then be compared to the reference dose obtained with the comprehensive set to see whether the underestimation of the peak dose is acceptable.

Because criterion S_2 in the approach for selecting safety-relevant radionuclides is different for sedimentary and fractured crystalline host formations, two separate PA models are developed for this validation exercise. The first model simulates the post-closure performance of a horizontal borehole repository constructed in an argillaceous formation; the second model considers a vertical borehole repository in fractured crystalline bedrock. The two models are described in detail in Finsterle et al. (2020) and Finsterle et al. (2021b), respectively; only a brief summary is provided here. In this approach, we combine key FEPs, multiple repository components on different scales, and simulation phases on different time scales into a single, integrated model, thus avoiding the need to establish links among numerous submodels or abstractions thereof that may be conceptually disparate or inconsistent with each other.

The model simulates fluid flow coupled to conductive and convective heat transfer, as well as advective and diffusive radionuclide transport, accounting for decay and ingrowth. The main repository components are explicitly represented, including the waste form, canister, annulus, casing, cement, drilling disturbed zone (DDZ), plugs, access structure, near field, geosphere, and the accessible environment. Processes in the biosphere are summarily represented by a dose conversion factor (ICRP, 2012).

After canister breach (assumed to occur 10,000 years after waste emplacement) and the mobilization of the inventory's instant release fraction (Nagra, 2002), a radiological source-term model (Finsterle et al., 2025a) calculates the congruent release of radionuclides encapsulated in the waste form. Decay heat is released from each canister using data by Ansolabehere et al. (2003). Key features of the geosphere include the host rock, which—for the horizontal borehole repository—is represented as an equivalent porous medium intersected by undetected or reactivated fault zones, or—for the vertical borehole repository—as a fracture network embedded in a granitic rock matrix. The host rock is in contact with a sedimentary overburden, which in turn underlies a near-surface freshwater aquifer, from which drinking water is extracted from a well.

Fluid flow is driven by a vertically upward head gradient and (for the vertical borehole repository model) topographic recharge-discharge effects. Temperatures follow the geothermal gradient; they change with time due to the heat-generating waste. Thermal expansion and contraction of the fluid and pore space lead to pressure and buoyancy effects, which are moderated at depth by the higher density of saline groundwater. Radionuclide concentrations evolve as a function of the time-dependent release from the canisters, radioactive decay and ingrowth, molecular diffusion, advective transport, and mixing. Radionuclide migration is retarded by reversible, linear adsorption, with adsorption coefficients for clay taken from Nagra (2002) and for crystalline bedrock from Carbol and Engkvist (1997). The model does not simulate kinetic dissolution, precipitation, or sorption processes. In fractured host rocks, radionuclide transport is further delayed by matrix diffusion effects, which are calculated based on the fracture network geometry, fracture density, and a utilization factor (Neretnieks, 1980). Following a near-steady initialization phase, predictive simulations cover a time frame that starts with waste emplacement, followed by the thermal period, and a long-term migration phase to 10 million years, i.e., beyond the time the peak dose is reached.

Figure 1 is a visualization of the integrated PA models. A two-dimensional, axial-radial discretization scheme is used for the near-field model, which is visualized in Figure 1A for a short segment of the 1 km long disposal section, showing two of the 200 individually represented canisters. This reduction in dimension is justified because the geometry of all components of the EBS and the near field (i.e., waste form, canister, annulus, casing, cement, and DDZ) are cylindrical, so are the key flow and transport processes (radial for heat conduction and diffusive radionuclide transport, and axial for fluid flow, heat convection, and advective radionuclide transport). This cylindrical source-term and near-field model is embedded into a conventional, three-dimensional model of the geosphere, using an unstructured Voronoi finite-volume grid. The computational meshes for the horizontal and vertical borehole repository models are shown in Figures 1B,C, respectively.

Radionuclide migration through crystalline bedrock is dominated by advective transport within the connected fracture network, retarded by matrix diffusion. This system is represented by a dual-continuum model with a depth-dependent trend of average fracture-network permeability (Achtziger-Zupančič et al., 2017) superimposed by geostatistically generated, spatially correlated and anisotropic variability (see Figure 1B). By contrast, radionuclide transport in tight clay formations is diffusion-dominated. As porosity influences the effective diffusion coefficient, a heterogeneous porosity field is generated (see Figure 1C). In addition, two subvertical faults intersect the disposal section of the repository, pressurizing the borehole and providing fast flow pathways to the land surface; for details, see Finsterle et al. (2021a).

The computational grid for representing the horizontal borehole repository consists of 42,024 elements and 119,306 connections between them; the dual-permeability model for the vertical borehole repository has 148,344 elements and 354,827 connections. The number of balance equations to be solved is equal to the number of radionuclides tracked in the model plus an equation for water, brine, and heat. For example, to simulate the 4N + 2 actinide decay chain for a repository in fractured granite, the degree of freedom is $(10 + 3) \times 148,344 = 1,928,472$, i.e., almost 2 million unknowns need to be determined simultaneously using Newton-Raphson iterations. The elements of the Jacobian matrix are calculated numerically. The set of linear equations arising at each Newton-Raphson iteration is inverted using an iterative sparse matrix solver. For this validation exercise, we use an extended version of the TOUGH2 nonisothermal flow and transport code (Pruess et al., 2012; Finsterle, 2021) as implemented in the iTOUGH2 simulation-optimization framework (Finsterle et al., 2017).

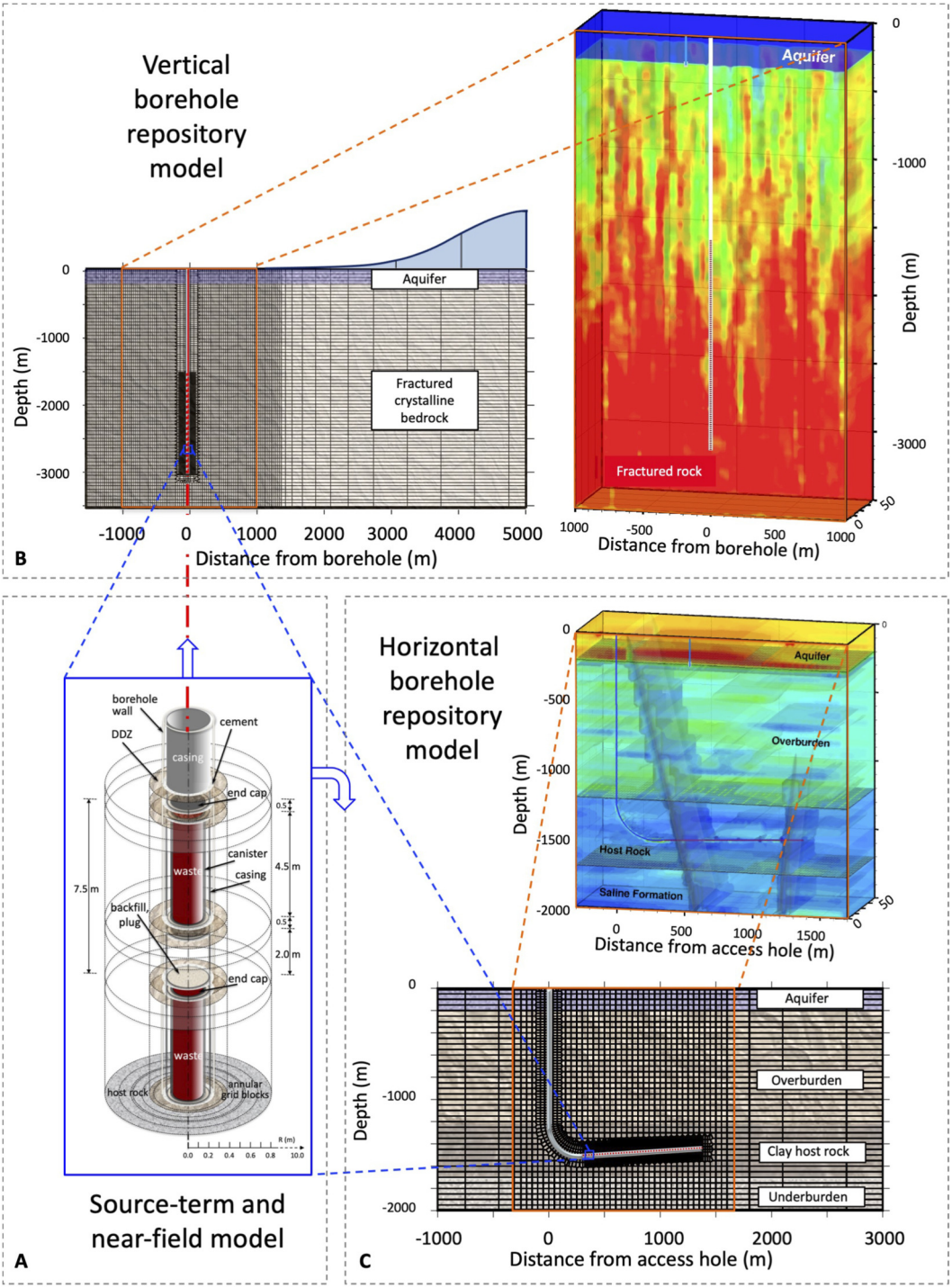

FIGURE 1
(A) Cylindrical near-field model embedded in **(B)** dual-permeability model of vertical borehole repository in fractured granite, and **(C)** model of horizontal borehole repository in clay host rock.

Note that if volatile radionuclides (such as ^{14}C and ^{3}H) are present in the waste inventory, they are included in the screening analysis. Calculating the transport of these volatile radionuclides in the gas phase (potentially driven by corrosion gas generation) is the purpose of a PA model that includes or is specifically designed to study this mechanism. For the deep borehole repositories chosen here for the validation exercise, transport of volatile radionuclides in a free gas phase is irrelevant, as demonstrated in Finsterle et al. (2025b). Consequently, the screening model did not select ^{14}C and ^{3}H as safety-relevant radionuclides for the two cases studied in this paper (see Section 3.1 below).

A very large number of geometrical, thermal, hydrological, and transport parameters define the repository design, material properties, initial and boundary conditions, and source terms of

TABLE 1 Parameters for selection of safety-relevant radionuclides.

Parameter	Value	Source/Comment
Inventory (kg/canister)	see Figure 2	Carter et al. (2012); SNF from PWR; initial enrichment: 4.73%; burn-up: 60 GWd/MTHM; converted from Bq/MTHM to kg/canister assuming 435 kg MTHM per PWR assembly (SNL, 2013) and one assembly per canister
Dose coefficient, dcf_i (Sv/Bq)	see Figure 2	ICRP (2012); for ingestion; radionuclide-specific
Sorption coefficient, K_d (m^3/kg)		Radionuclide and formation specific
Argillaceous host rock	see Figure 2	Nagra (2002); Opalinus clay
Crystalline host rock	see Figure 3	Carbol and Engkvist (1997); Äspö diorite
Porosity (m^3/m^3)		
Argillaceous formation ϕ	0.100	
Crystalline formation: fractures, ϕ_f	0.001	
matrix, ϕ_m	0.010	
Cement ϕ_c	0.100	
Accessible porosity factor, ϵ (–)	see Figure 2	Nagra (2002); 0.5 for anions and 1 for non-anions
Canister breach time, t_b (years)	10,000	
Diffusive transport distance, L_{diff} (m)		Equation 4
Argillaceous formation	200	Half-thickness of host formation
Crystalline formation	0.1	Thickness of borehole annulus
Fracture spacing, S (m)	100	Utilization factor for matrix diffusion: $\psi = 2\eta/S$
Penetration distance, η (m)	20	
Effective diffusion coefficient, Σ (m^2/s)	10^{-9}	Equation 4, Millington and Quirk (1961)
Advective transport distance, L_{adv} (m)		Equation 5
Argillaceous formation	1,000	Thickness of overburden
Crystalline formation	2,000	Mid-depth of repository to aquifer
Head gradient, ∇H (m/m)	0.01	Equation 5
Hydraulic conductivity, K (m/s)		
Argillaceous formation	10^{-10}	
Crystalline formation	10^{-8}	Fracture network continuum

these two models. The chosen values are representative of borehole repositories at a generic disposal site; they are listed in Finsterle et al. (2020), Finsterle et al. (2021a), Finsterle et al. (2021b). Note that the purpose of the simulations presented in Section 3.2 below is not to assess repository performance, but to examine the relative contributions of individual radionuclides to the total peak exposure dose, and to determine whether the most safety-relevant parameters were appropriately pre-selected by the approach described in Section 2.1.

3 Results and discussion

3.1 Selection of safety-relevant radionuclides

The radionuclide selection approach described in Section 2.1 is applied to the inventory reported for a once-through fuel cycle of a commercial SNF assembly from a PWR reactor (Carter et al., 2012). Additional assumptions and parameters used for the calculation of the screening scores are summarized in Table 1.

Figure 2 shows an excerpt from the spreadsheet used to identify the safety-relevant radionuclides for SNF assemblies disposed in a horizontal borehole repository sited in a clay formation. For each radioisotope present in the waste form, radionuclide-specific properties (half-life, specific activity, and dose conversion factor, shown in grey) are compiled. The total inventory of each radionuclide (shown in green) is the sum of the initial inventory at the reference time and the contributions from ingrowth from the actinide decay chains, calculated using Equation 2. Note that radionuclides in decay-chain branches with very low branching ratios or very short half-lives are not explicitly tracked; however, their dose contribution is included in the dose conversion factor.

Based on this initial input, the first score, S_1 of Equation 1, is evaluated, normalized, ranked, and truncated using a threshold value of 10^{-6}, resulting in a reduction of the initial set of 51 radionuclides present in the waste form to a set of 17 potentially safety-relevant radionuclides (see radionuclides

10.3389/fnuen.2026.1787346

Radio-nuclide	Halflife $t_{1/2}$ (years)	Specific activity a (Bq/kg)	Dose coef. dcf (Sv/Bq)	Inven-tory m_0 (kg/can)	In-growth $m_{0'}$ (kg/can)	Total invent. m (kg/can)	S1 norm (-)	Select 1 $>10^{-6}$ (-)	Sorp-tion K_d (m^3/kg)	Access. porosity ε (-)	Retard. sorpt. R_{sorb} (-)	Retard. diffu. R_{diff} (-)	S2 norm (-)	Select 2 >1E-3 (-)
I-129	1.6E+07	6.4E+09	1.1E-07	1.4E-01	0.0E+00	1.4E-01	3.5E-02	3.5E-02	3.0E-05	5.0E-01	1.4E+00	1.0E+00	1.0E+00	I-129
Se-79	3.3E+05	5.1E+11	2.9E-09	4.6E-03	0.0E+00	4.6E-03	4.3E-04	4.3E-04	0.0E+00	5.0E-01	1.0E+00	1.0E+00	1.3E-02	Se-79
Cl-36	3.0E+05	1.2E+12	9.3E-10	2.2E-04	0.0E+00	2.2E-04	1.3E-05	1.3E-05	0.0E+00	5.0E-01	1.0E+00	1.0E+00	3.9E-04	
Th-232	1.4E+10	4.1E+06	2.3E-07	6.8E-07	1.1E-01	1.1E-01	4.1E-05	4.1E-05	5.0E+01	1.0E+00	1.3E+06	1.0E+00	2.0E-26	
U-238	4.5E+09	1.2E+07	4.5E-08	4.0E+02	6.3E-01	4.0E+02	8.6E-02	8.6E-02	2.0E+01	1.0E+00	5.0E+05	1.0E+00	4.9E-29	
U-235	7.0E+08	8.0E+07	4.7E-08	2.3E+00	3.4E+00	5.7E+00	8.4E-03	8.4E-03	2.0E+01	1.0E+00	5.0E+05	1.0E+00	0.0E+00	
Zr-93	1.6E+06	8.8E+10	1.1E-09	6.4E-01	0.0E+00	6.4E-01	1.7E-02	1.7E-02	1.0E+01	1.0E+00	2.5E+05	1.0E+00	0.0E+00	
Tc-99	2.1E+05	6.3E+11	6.4E-10	5.6E-01	0.0E+00	5.6E-01	5.3E-03	5.3E-03	5.0E+01	1.0E+00	1.3E+06	1.0E+00	0.0E+00	
Pd-107	6.5E+06	1.9E+10	3.7E-11	1.8E-01	0.0E+00	1.8E-01	4.5E-05	4.5E-05	5.0E+01	1.0E+00	1.3E+06	1.0E+00	0.0E+00	
Sn-126	2.3E+05	4.6E+11	4.7E-09	2.2E-02	0.0E+00	2.2E-02	1.4E-03	1.4E-03	1.0E+02	1.0E+00	2.5E+06	1.0E+00	0.0E+00	
Cs-135	1.3E+06	7.4E+10	2.0E-09	3.4E-01	0.0E+00	3.4E-01	1.2E-02	1.2E-02	5.0E-01	1.0E+00	1.3E+04	1.0E+00	0.0E+00	
Th-230	7.5E+04	7.6E+11	2.1E-07	2.2E-06	1.3E-01	1.3E-01	3.2E-03	3.2E-03	5.0E+01	1.0E+00	1.3E+06	1.0E+00	0.0E+00	
U-233	1.6E+05	3.6E+11	5.1E-08	2.0E-06	1.7E-01	1.7E-01	3.0E-02	3.0E-02	2.0E+01	1.0E+00	5.0E+05	1.0E+00	0.0E+00	
U-234	2.5E+05	2.3E+11	4.9E-08	8.7E-02	5.3E-02	1.4E-01	5.5E-02	5.5E-02	2.0E+01	1.0E+00	5.0E+05	1.0E+00	0.0E+00	
U-236	2.3E+07	2.4E+09	4.7E-08	2.7E+00	1.8E+00	4.5E+00	1.9E-01	1.9E-01	2.0E+01	1.0E+00	5.0E+05	1.0E+00	0.0E+00	
Np-237	2.1E+06	2.6E+10	1.1E-07	5.2E-01	1.9E-01	7.1E-01	6.0E-01	6.0E-01	5.0E+01	1.0E+00	1.3E+06	1.0E+00	0.0E+00	
Pu-242	3.8E+05	1.5E+11	2.4E-07	3.6E-01	2.3E-03	3.6E-01	1.0E+00	1.0E+00	2.0E+01	1.0E+00	5.0E+05	1.0E+00	0.0E+00	
Ni-59	7.6E+04	3.0E+12	6.3E-11	2.2E-02	0.0E+00	2.2E-02	6.8E-07							
Be-10	1.4E+06	9.5E+11	1.1E-09	1.8E-07	0.0E+00	1.8E-07	4.7E-08							
Pa-231	3.3E+04	1.7E+12	7.1E-07	3.9E-07	4.8E-03	4.8E-03	3.4E-08							
Pu-239	2.4E+04	2.3E+12	2.5E-07	3.2E+00	1.2E-01	3.3E+00	1.7E-08							
Ca-41	1.0E+05	3.1E+12	1.9E-10	1.1E-06	0.0E+00	1.1E-06	8.2E-10							
Th-229	7.9E+03	7.3E+12	4.9E-07	2.4E-09	1.6E-01	1.6E-01	9.0E-31							
Cm-245	8.3E+03	6.5E+12	2.1E-07	4.2E-03	0.0E+00	4.2E-03	1.9E-31							
Am-243	7.3E+03	7.4E+12	2.0E-07	1.2E-01	5.2E-04	1.2E-01	8.9E-34							
Pu-240	6.6E+03	8.4E+12	2.5E-07	1.7E+00	6.1E-02	1.8E+00	1.3E-36							
C(io)-14	5.7E+03	1.6E+14	5.8E-10	2.0E-04	0.0E+00	2.0E-04	1.4E-47							
Cm-246	4.8E+03	1.1E+13	2.1E-07	8.2E-04	0.0E+00	8.2E-04	1.0E-54							
Mo-93	4.8E+03	3.0E+13	3.1E-09	1.3E-05	0.0E+00	1.3E-05	2.0E-57							
Ra-226	1.6E+03	3.7E+13	2.8E-07	1.1E-10	1.3E-01	1.3E-01	0.0E+00							
Ho(m)-166	1.2E+03	6.6E+13	1.4E-09	2.9E-06	0.0E+00	2.9E-06	0.0E+00							
H-3	1.2E+01	3.6E+17	1.8E-11	4.1E-05	0.0E+00	4.1E-05	0.0E+00							
Ni-63	1.0E+02	2.1E+15	1.5E-10	4.5E-03	0.0E+00	4.5E-03	0.0E+00							
Sr-90	2.9E+01	5.1E+15	2.8E-08	3.5E-01	0.0E+00	3.5E-01	0.0E+00							
Nb(m)-93	1.6E+01	8.8E+15	1.2E-10	1.8E-06	0.0E+00	1.8E-06	0.0E+00							
Ag(m)-108	4.2E+02	2.9E+14	2.3E-09	3.1E-07	0.0E+00	3.1E-07	0.0E+00							
Cs-137	3.0E+01	3.2E+15	1.3E-08	8.1E-01	0.0E+00	8.1E-01	0.0E+00							
Sm-151	9.5E+01	9.3E+14	9.8E-11	9.4E-03	0.0E+00	9.4E-03	0.0E+00							
Pb-210	2.2E+01	2.8E+15	6.9E-07	2.3E-13	1.2E-01	1.2E-01	0.0E+00							
Po-210	3.8E-01	1.7E+17	1.2E-06	4.7E-13	1.2E-01	1.2E-01	0.0E+00							
Ac-227	2.2E+01	2.7E+15	1.1E-06	4.7E-11	4.7E-03	4.7E-03	0.0E+00							
Ra-228	5.8E+00	1.0E+16	6.9E-07	1.1E-16	2.0E-06	2.0E-06	0.0E+00							
Th-228	1.9E+00	3.0E+16	7.2E-08	3.9E-08	4.7E-06	4.7E-06	0.0E+00							
U-232	6.9E+01	8.3E+14	3.3E-07	3.0E-08	1.1E-01	1.1E-01	0.0E+00							
Pu-238	8.8E+01	6.3E+14	2.3E-07	2.6E-01	2.4E-01	5.0E-01	0.0E+00							
Am-241	4.3E+02	1.3E+14	2.0E-07	1.8E-01	4.2E-03	1.8E-01	0.0E+00							
Pu-241	1.4E+01	3.8E+15	4.8E-09	5.5E-01	5.7E-03	5.5E-01	0.0E+00							
Am(m)-242	1.4E+02	3.9E+14	1.9E-07	1.4E-03	8.3E-04	2.3E-03	0.0E+00							
Cm-243	2.9E+01	1.9E+15	1.5E-07	5.0E-04	0.0E+00	5.0E-04	0.0E+00							
Cm-244	1.8E+01	3.0E+15	1.2E-07	6.0E-02	0.0E+00	6.0E-02	0.0E+00							

FIGURE 2
Selection of safety-relevant radionuclides for PWR SNF disposed in a horizontal borehole repository sited in a shale formation. Radionuclides printed in pink are part of an actinide decay chain.

printed in red and blue in Figure 2). These radionuclides are expected to have the highest peak dose if their transport from the repository to the biosphere were not retarded by sorption.

For the second screening step, the sorption coefficients and accessible porosities are needed to estimate the retardation factor R_{Kd} (Equation 6), and to evaluate the second score S_2 of Equation 9. Using a threshold value of 10^{-3}, 15 of the 17 remaining radionuclides are screened out, leaving ^{129}I and ^{79}Se as the isotopes that likely dominate peak exposure dose. The third screening step S_3, which is based on the solubility limit (see Equation 10), is not invoked, as the solubility limit of ^{129}I is very high, and that of ^{79}Se depends strongly on the actual speciation of selenium in the waste form and near-field environment. As discussed in Section 2.1, the calculation of the near-field concentrations to determine whether they exceed the solubility limit is fraught with conceptual difficulties; the S_3 criterion should therefore only be used after careful consideration. As the current

number of safety-relevant radionuclides is small and thus already manageable, it is preferable to conservatively assume that ^{79}Se is not solubility-limited.

The selection process suggests that including ^{129}I and ^{79}Se in a computationally demanding PA model will provide peak dose estimates that are close to the value that would be obtained if all 51 radionuclides present in the SNF were tracked in the model. The peak dose will be underestimated by less than about 0.1%, i.e., the order of the second threshold criterion of 10^{-3}. Also recall that the screening process estimates the relative peak dose of individual radionuclides rather than the total peak dose of all radionuclides, which is likely lower than the sum of all individual peak dose values as they occur at different times. The threshold value can be adjusted to reflect the required accuracy of the simulation. For example, if the selection criterion had been reduced from 10^{-3} to 10^{-4}, ^{36}Cl would need to be included in the set of potentially safety-relevant radionuclides, improving the prediction of the total peak dose at the expense of increased computational demands.

Figure 3 shows the equivalent information for a deep borehole repository in crystalline bedrock. In the first down-selection step based on the S_1 score, a few comparatively short-lived radionuclides are included—unlike for a repository in an argillaceous formation—because the advection-dominated transport time through the fracture network to the biosphere is much shorter; recall that the retardation effect due to matrix diffusion is not included in this first step.

The calculation of the S_2 score is different as the retardation factor in a fractured host formation includes matrix diffusion effects estimated using Equation 8. Because all radionuclides migrate by advective transport through the fracture network, and since matrix diffusion retards also non-sorbing radionuclides, the S_2 scores are less differentiated, and a larger number of radionuclides pass the 10^{-3} selection criterion. In addition to the fission products ^{99}Tc, ^{129}I, and ^{79}Se, the actinides ^{236}U, ^{238}U, ^{235}U, and ^{237}Np are potentially safety relevant. ^{99}Tc is identified as the most safety-relevant radionuclide mainly because of the assumption that it is under the redox state Tc(VII) in saline groundwater and therefore non-sorbing (Carbol and Engkvist, 1997). Assigning even a small K_d value would sufficiently retard the migration of ^{99}Tc for it not to be a safety concern. Note that the four safety-relevant actinides are not only radionuclides with high initial inventories in the waste form, but they are also the daughter product in one of the actinide decay chains (see Figure 4). While the estimated ingrowth amount is added to the initial inventory for the screening calculation, all parent radionuclides that lead to a safety-relevant daughter product need to be included in the high-fidelity PA model, unless the ingrowth is considered an insignificant fraction of the initial inventory.

To illustrate the application of this rule, consider the list of safety-relevant radionuclides identified for the vertical borehole repository, as shown in Figure 3. Four of these radionuclides (^{236}U, ^{238}U, ^{235}U, and ^{237}Np) are daughter products of the actinide decay chains; they are highlighted in orange in Figure 4. All parent products above the safety-relevant daughter product contribute to the mass of the safety-relevant daughter; they are printed in pink. Figure 4 also reveals that the mass generated by ingrowth is either larger than or a significant fraction (i.e., greater than the screening criterion of 0.001) of the mass initially present in the waste form. Consequently, all radionuclides printed in pink should be tracked in the high-fidelity PA model.

As a byproduct, the proposed screening approach directly reveals the impact of changing the threshold value. Because the radionuclides in the inventory are already ranked according to the normalized S_2 score, the list of safety-relevant radionuclides can immediately me gleaned from the table for *any* threshold value. For example, in Figure 4, the threshold would have to be lowered from 10^{-3} to 10^{-8} before the next radionuclide (^{129}Sn) makes the cut and needs to be included in the PA model. Conversely, increasing the threshold value to 10^{-2} would classify ^{79}Se and ^{237}Np as non-safety-relevant, and a threshold value of 0.1 would result in a set of only two radionuclides, ^{99}Tc and ^{129}I. Some guidance on the choice of the threshold value has been given in Section 2.1.

3.2 Validation of radionuclide screening approach

To test whether the proposed screening approach identifies a sensible subset of radionuclides that yields sufficiently accurate predictions of peak exposure dose, we compare results obtained by a PA model that tracks only safety-relevant radionuclides with those from a model that includes a comprehensive set of radionuclides. If the differences in peak dose values calculated with the reduced and comprehensive sets are acceptably small, the screening approach described in Section 2.1 and exercised as discussed in Section 3.1 can be considered reasonable according to the tenets of pragmatic model validation (Finsterle and Lanyon, 2022). It is important to note that the list of safety-relevant radionuclides derived in Section 3.1 as well as the resulting dose curves (presented in Figures 5, 6 below) are specific to the waste forms, disposal concept, geologic environment, and scenario chosen for this validation exercise. Nevertheless, the proposed screening approach is applicable to a wide variety of disposal pathways and analysis scenarios by selecting the appropriate, system-specific values for the screening factors.

We first present this comparison for the horizontal borehole repository in an argillaceous formation, where ^{129}I and ^{79}Se have been identified as the most safety-relevant radionuclides. The PA model is run with a total of 34 radionuclides, which include those passing the S_1 and S_2 selection criteria (highlighted in red and blue in Figure 2) and the members of the four actinide series shown in Figure 4.

Figure 5 shows the breakthrough curves of radionuclides with a peak dose exceeding 10^{-10} mSv yr^{-1}. With the exception of ^{129}I and ^{79}Se—the two radionuclides identified as safety-relevant by the screening method—and ^{36}Cl—the third-highest-ranking isotope passing the S_1 criterion but being screened out by the S_2 criterion—the remaining 31 radionuclides have individual peak dose values that are smaller than 10^{-10} mSv yr^{-1}, i.e., below the standard of 0.1 mSv yr^{-1} by at least nine orders of magnitude. The sequence of the three radionuclides is consistent with the preliminary ranking estimated by the screening approach, with ^{129}I having the highest peak dose of 5.4×10^{-3} mSv kg^{-1}, followed by ^{79}Se with 1.4×10^{-5} mSv kg^{-1} and ^{36}Cl with 4.2×10^{-7} mSv kg^{-1}. A common characteristic of these three radionuclides is that they are non-sorbing on clay minerals and thus highly mobile.

10.3389/fnuen.2026.1787346

Radio-nuclide	Halflife $t_{1/2}$ (years)	Specific activity a (Bq/kg)	Dose coef. dcf (Sv/Bq)	Inven-tory m_0 (kg/can)	In-growth $m_{0'}$ (kg/can)	Total invent. m (kg/can)	S1 norm (-)	Select 1 >1E-6 (-)	Sorp-tion K_d (m^3/kg)	Access. porosity ε (-)	Retard. sorpt. R_{sorb} (-)	Retard. diffu. R_{diff} (-)	S2 norm (-)	Select 2 >1E-3 (-)
Tc-99	2.1E+05	6.3E+11	6.4E-10	5.6E-01	0.0E+00	5.6E-01	1.5E-04	1.5E-04	0.0E+00	1.0E+00	1.0E+00	5.0E+00	1.0E+00	Tc-99
I-129	1.6E+07	6.4E+09	1.1E-07	1.4E-01	0.0E+00	1.4E-01	6.6E-05	6.6E-05	0.0E+00	5.0E-01	1.0E+00	3.0E+00	5.0E-01	I-129
U-236	2.3E+07	2.4E+09	4.7E-08	2.7E+00	1.8E+00	4.5E+00	3.6E-04	3.6E-04	5.0E-03	1.0E+00	5.4E+02	5.0E+00	4.1E-01	U-236
U-238	4.5E+09	1.2E+07	4.5E-08	4.0E+02	6.3E-01	4.0E+02	1.5E-04	1.5E-04	5.0E-03	1.0E+00	5.4E+02	5.0E+00	1.8E-01	U-238
U-235	7.0E+08	8.0E+07	4.7E-08	2.3E+00	3.4E+00	5.7E+00	1.5E-05	1.5E-05	5.0E-03	1.0E+00	5.4E+02	5.0E+00	1.7E-02	U-235
Np-237	2.1E+06	2.6E+10	1.1E-07	5.2E-01	1.9E-01	7.1E-01	1.4E-03	1.4E-03	5.0E-03	1.0E+00	5.4E+02	5.0E+00	1.6E-03	Np-237
Se-79	3.3E+05	5.1E+11	2.9E-09	4.6E-03	0.0E+00	4.6E-03	4.6E-06	4.6E-06	1.0E-03	5.0E-01	5.5E+01	3.0E+00	1.1E-03	Se-79
Sn-126	2.3E+05	4.6E+11	4.7E-09	2.2E-02	0.0E+00	2.2E-02	3.1E-05	3.1E-05	1.0E-03	1.0E+00	1.1E+02	5.0E+00	1.6E-08	
U-234	2.5E+05	2.3E+11	4.9E-08	8.7E-02	5.3E-02	1.4E-01	1.1E-03	1.1E-03	5.0E-03	1.0E+00	5.4E+02	5.0E+00	3.6E-33	
Cs-135	1.3E+06	7.4E+10	2.0E-09	3.4E-01	0.0E+00	3.4E-01	3.4E-05	3.4E-05	5.0E-02	1.0E+00	5.4E+03	5.0E+00	8.6E-63	
U-233	1.6E+05	3.6E+11	5.1E-08	2.0E-06	1.7E-01	1.7E-01	2.1E-03	2.1E-03	1.0E-02	1.0E+00	1.1E+03	5.0E+00	0.0E+00	
C(io)-14	5.7E+03	1.6E+14	5.8E-10	2.0E-04	0.0E+00	2.0E-04	3.9E-06	3.9E-06	1.0E-03	1.0E+00	1.1E+02	5.0E+00	0.0E+00	
Ni-59	7.6E+04	3.0E+12	6.3E-11	2.2E-02	0.0E+00	2.2E-02	2.6E-06	2.6E-06	3.0E+00	1.0E+00	3.2E+05	5.0E+00	0.0E+00	
Zr-93	1.6E+06	8.8E+10	1.1E-09	6.4E-01	0.0E+00	6.4E-01	4.3E-05	4.3E-05	1.0E+00	1.0E+00	1.1E+05	5.0E+00	0.0E+00	
Ra-226	1.6E+03	3.7E+13	2.8E-07	1.1E-10	1.3E-01	1.3E-01	1.1E-02	1.1E-02	2.0E-02	1.0E+00	2.2E+03	5.0E+00	0.0E+00	
Th-229	7.9E+03	7.3E+12	4.9E-07	2.4E-09	1.6E-01	1.6E-01	1.7E-01	1.7E-01	5.0E+00	1.0E+00	5.4E+05	5.0E+00	0.0E+00	
Th-230	7.5E+04	7.6E+11	2.1E-07	2.2E-06	1.3E-01	1.3E-01	1.3E-02	1.3E-02	5.0E+00	1.0E+00	5.4E+05	5.0E+00	0.0E+00	
Pa-231	3.3E+04	1.7E+12	7.1E-07	3.9E-07	4.8E-03	4.8E-03	3.3E-03	3.3E-03	1.0E+00	1.0E+00	1.1E+05	5.0E+00	0.0E+00	
Pu-239	2.4E+04	2.3E+12	2.5E-07	3.2E+00	1.2E-01	3.3E+00	1.0E+00	1.0E+00	5.0E+00	1.0E+00	5.4E+05	5.0E+00	0.0E+00	
Pu-240	6.6E+03	8.4E+12	2.5E-07	1.7E+00	6.1E-02	1.8E+00	9.1E-01	9.1E-01	5.0E+00	1.0E+00	5.4E+05	5.0E+00	0.0E+00	
Pu-242	3.8E+05	1.5E+11	2.4E-07	3.6E-01	2.3E-03	3.6E-01	8.5E-03	8.5E-03	5.0E+00	1.0E+00	5.4E+05	5.0E+00	0.0E+00	
Am-243	7.3E+03	7.4E+12	2.0E-07	1.2E-01	5.2E-04	1.2E-01	4.7E-02	4.7E-02	3.0E+00	1.0E+00	3.2E+05	5.0E+00	0.0E+00	
Cm-245	8.3E+03	6.5E+12	2.1E-07	4.2E-03	0.0E+00	4.2E-03	1.7E-03	1.7E-03	3.0E+00	1.0E+00	3.2E+05	5.0E+00	0.0E+00	
Cm-246	4.8E+03	1.1E+13	2.1E-07	8.2E-04	0.0E+00	1.9E-03	7.2E-04	7.2E-04	3.0E+00	1.0E+00	3.2E+05	5.0E+00	0.0E+00	
Am-241	4.3E+02	1.3E+14	2.0E-07	1.8E-01	4.2E-03	1.8E-01	3.2E-07							
Mo-93	4.8E+03	3.0E+13	3.1E-09	1.3E-05	0.0E+00	1.3E-05	2.0E-07							
Cl-36	3.0E+05	1.2E+12	9.3E-10	2.2E-04	0.0E+00	2.2E-04	1.7E-07							
Pd-107	6.5E+06	1.9E+10	3.7E-11	1.8E-01	0.0E+00	1.8E-01	8.8E-08							
Th-232	1.4E+10	4.1E+06	2.3E-07	6.8E-07	1.1E-01	1.1E-01	7.3E-08							
Ho(m)-166	1.2E+03	6.6E+13	1.4E-09	2.9E-06	0.0E+00	2.9E-06	5.6E-10							
Ca-41	1.0E+05	3.1E+12	1.9E-10	1.1E-06	0.0E+00	1.1E-06	4.2E-10							
Be-10	1.4E+06	9.5E+11	1.1E-09	1.8E-07	0.0E+00	1.8E-07	1.3E-10							
Ag(m)-108	4.2E+02	2.9E+14	2.3E-09	3.1E-07	0.0E+00	3.1E-07	8.2E-15							
Am(m)-242	1.4E+02	3.9E+14	1.9E-07	1.4E-03	8.3E-04	2.3E-03	5.1E-23							
Pu-238	8.8E+01	6.3E+14	2.3E-07	2.6E-01	2.4E-01	5.0E-01	1.4E-33							
Ni-63	1.0E+02	2.1E+15	1.5E-10	4.5E-03	0.0E+00	4.5E-03	5.3E-34							
Sm-151	9.5E+01	9.3E+14	9.8E-11	9.4E-03	0.0E+00	9.4E-03	5.5E-36							
U-232	6.9E+01	8.3E+14	3.3E-07	3.0E-08	1.1E-01	1.1E-01	2.2E-43							
Cs-137	3.0E+01	3.2E+15	1.3E-08	8.1E-01	0.0E+00	8.1E-01	0.0E+00							
Sr-90	2.9E+01	5.1E+15	2.8E-08	3.5E-01	0.0E+00	3.5E-01	0.0E+00							
Cm-243	2.9E+01	1.9E+15	1.5E-07	5.0E-04	0.0E+00	5.0E-04	0.0E+00							
Pb-210	2.2E+01	2.8E+15	6.9E-07	2.3E-13	1.2E-01	1.2E-01	0.0E+00							
Ac-227	2.2E+01	2.7E+15	1.1E-06	4.7E-11	4.7E-03	4.7E-03	0.0E+00							
Cm-244	1.8E+01	3.0E+15	1.2E-07	6.0E-02	0.0E+00	6.0E-02	0.0E+00							
Nb(m)-93	1.6E+01	8.8E+15	1.2E-10	1.8E-06	0.0E+00	1.8E-06	0.0E+00							
Pu-241	1.4E+01	3.8E+15	4.8E-09	5.5E-01	5.7E-03	5.5E-01	0.0E+00							
H-3	1.2E+01	3.6E+17	1.8E-11	4.1E-05	0.0E+00	4.1E-05	0.0E+00							
Po-210	3.8E-01	1.7E+17	1.2E-06	4.7E-13	1.2E-01	1.2E-01	0.0E+00							
Ra-228	5.8E+00	1.0E+16	6.9E-07	1.1E-16	2.0E-06	2.0E-06	0.0E+00							
Th-228	1.9E+00	3.0E+16	7.2E-08	3.9E-08	4.7E-06	4.7E-06	0.0E+00							

FIGURE 3
Selection of safety-relevant radionuclides for PWR SNF disposed in a vertical borehole repository sited in a fractured granite formation. Radionuclides printed in pink are part of an actinide decay chain.

Essentially all the remaining radionuclides of the comprehensive set, including those from the actinide decay chains, have sufficiently high sorption coefficients so they are considerably retarded, or they have a very low product of inventory, half-life, and dose conversion factor. As a result, their concentrations in the near-surface aquifer used as a source of drinking water are very low, and their contribution to peak dose is negligible.

Adding the dose contribution from ^{36}Cl to those of the two safety-relevant radionuclides ^{129}I and ^{79}Se leads to an increase in the peak dose by about 0.002%, which is insignificant given the uncertainty in the predicted peak dose, which is likely many orders of magnitude higher due to epistemic and aleatoric uncertainties inherent in the conceptual and numerical PA model, as demonstrated by the results of sampling-based

10.3389/fnuen.2026.1787346

Actinide Decay Chains			
Decay chain Radionuclide	Inventory (kg/UCS)	Ingrowth (kg/UCS)	Total (kg/UCS)
4N: Cm-244 --> 240-Pu --> U-236 --> U-232 --> Th-232 --> Ra-228 --> Th-228			
Cm-244	6.0E-02	0.0E+00	6.0E-02
Pu-240	1.7E+00	5.9E-02	1.8E+00
U-236	2.7E+00	1.8E+00	4.5E+00
U-232	3.0E-08	1.1E-01	1.1E-01
Th-232	6.8E-07	1.1E-01	1.1E-01
Ra-228	1.1E-16	4.5E-06	4.5E-06
Th-228	3.9E-08	4.5E-06	4.6E-06
4N+1: Cm-245 --> Am-241 --> Np-237 --> U-233 --> Th-229			
Cm-245	4.2E-03	0.0E+00	4.2E-03
Am-241	1.8E-01	4.1E-03	1.8E-01
Np-237	5.2E-01	1.8E-01	7.0E-01
U-233	2.0E-06	1.7E-01	1.7E-01
Th-229	2.4E-09	1.6E-01	1.6E-01
4N+2: Cm-246 --> Am-242m --> Pu-242 --> Pu-238 --> U-238 --> U-234 --> Th-230 --> Ra-226 --> Pb-210 --> Po-210			
Cm-246	8.2E-04	0.0E+00	8.2E-04
Am(m)-242	1.4E-03	8.0E-04	2.2E-03
Pu-242	3.6E-01	2.2E-03	3.6E-01
Pu-238	2.6E-01	3.5E-01	6.1E-01
U-238	4.0E+02	6.1E-01	4.0E+02
U-234	8.7E-02	5.2E-02	1.4E-01
Th-230	2.2E-06	1.2E-01	1.2E-01
Ra-226	1.1E-10	1.2E-01	1.2E-01
Pb-210	2.3E-13	1.1E-01	1.1E-01
Po-210	4.7E-13	1.1E-01	1.1E-01
4N+3: Cm-243 --> Am-243 --> Pu-239 --> U-235 --> Pa-231 --> Ac-227			
Cm-243	5.0E-04	0.0E+00	5.0E-04
Am-243	1.2E-01	5.0E-04	1.2E-01
Pu-239	3.2E+00	1.2E-01	3.3E+00
U-235	2.3E+00	3.3E+00	5.6E+00
Pa-231	3.9E-07	4.6E-03	4.6E-03
Ac-227	4.7E-11	4.6E-03	4.6E-03

FIGURE 4
Approximate calculation of ingrowth from the actinide decay chains. Actinides printed in pink need to be included in a performance assessment model for a vertical borehole repository as they contribute to the dose of a safety-relevant radionuclide (shaded in orange).

uncertainty propagation analyses for borehole repositories (Finsterle et al., 2020; Finsterle et al., 2025a).

Note that it would have been acceptable to also omit ^{79}Se, whose peak-dose contribution is only about 0.07%; ignoring ^{79}Se would have no impact on the conclusions about repository performance derived from the PA model. The screening approach estimated that the peak dose of ^{79}Se would be about 1.3% of that of ^{129}I (which is greater than the threshold value of 10^{-3}, making ^{79}Se pass the selection criteria). The safety-relevance of ^{79}Se is overrated because of the simplified calculation of the peak dose time t_t (see Equations 3–5); t_t of ^{79}Se is underestimated by more than its half-life. This issue could be mitigated by performing a second iteration of the screening process, in which t_t from the most safety-relevant radionuclide (here ^{129}I) is used rather than the peak dose times of each individual radionuclide. This would also account for the fact that the total peak dose is determined by the sum of the dose contributions at the time peak dose occurs, rather than the sum of the individual peak dose values, which occur at different times. While the time when the sum of all dose curves reaches its maximum cannot be calculated by the screening model, it is expected to occur around the time the most safety-relevant radionuclide reaches its highest value.

In summary, tracking 34 radionuclides present in SNF yields a total peak exposure dose that is essentially identical to that of ^{129}I, which was correctly identified by the simple screening approach as the most safety-relevant radionuclide for SNF disposal in a horizontal borehole repository in argillite. This confirms that the proposed screening approach provides a sensible selection of radionuclides to be tracked in a PA model that is based on a similar repository layout and similar assumptions about material

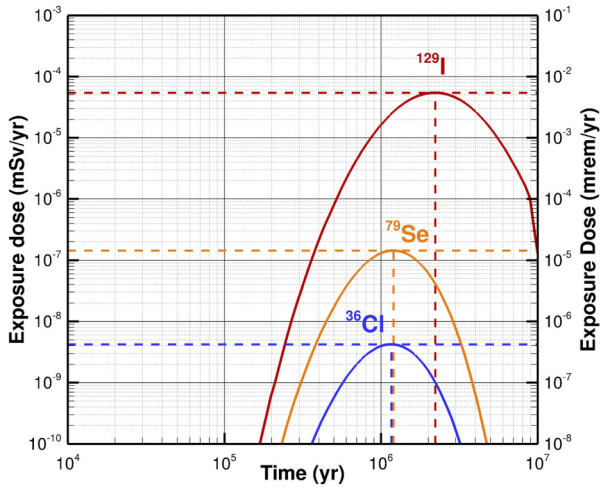

FIGURE 5
Exposure dose as a function of time for the two radionuclides (^{129}I and ^{79}Se) identified as safety-relevant for a horizontal borehole repository in an argillaceous host formation. ^{36}Cl is the non-selected radionuclide with the highest peak dose contribution. The total dose curve summing all 34 tracked radionuclides is only marginally higher than that of ^{129}I.

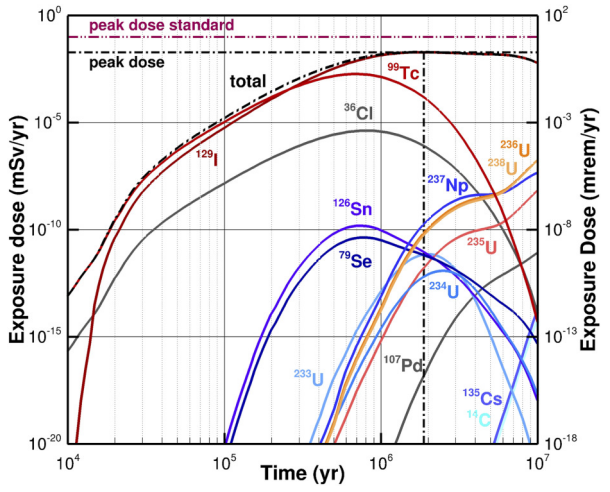

FIGURE 6
Exposure dose as a function of time for radionuclides tracked in the comprehensive PA model for a vertical borehole repository sited in fractured crystalline rock. Only 14 of the 36 tracked radionuclides exceed a peak dose of 10^{-20} mSv yr^{-1}.

properties as those used by the screening model (see Table 1 and grey columns in Figure 2).

As indicated above, SNF disposal in fractured rock leads to a larger set of potentially safety-relevant radionuclides because of comparatively fast advective transport through the fracture network (adding radionuclides with a shorter half-life to the list) and retardation by matrix diffusion, which is less discerning because diffusion coefficients are similar for all radionuclides. For this validation exercise, we also used conservatively low sorption coefficients to increase the number of radionuclides arriving at the drinking water well. Recall that this simulation study and the associated parameter choices are made for the purpose of validating the proposed screening approach, not to determine the safety of a particular repository type or scenario.

Figure 6 shows the dose curves for each radionuclide with a peak dose greater than 10^{-20} mSv yr^{-1}. Radionuclides identified as safety-relevant (^{99}Tc, ^{129}I, ^{236}U, ^{238}U, ^{235}U, ^{237}Np, and ^{79}Se) are shown in warm colors; those having passed the first but failed the second screening threshold (^{126}Sn, ^{234}U, ^{135}Cs, ^{14}C, ^{59}Ni, ^{93}Zr, ^{226}Ra, ^{229}Th, ^{230}Th, ^{231}Pa, ^{239}Pu, ^{240}Pu, ^{242}Pu, ^{243}Am, ^{245}Cm, ^{246}Cm) are shown in cold colors; the remaining radionuclides are shown in grey. The sum of the dose contributions from all 36 tracked radionuclides is shown as a dash-dotted black line, which reaches a peak dose of 0.02 mSv yr^{-1}, i.e., a factor of five below the dose standard. We first notice that the radionuclides with the highest S_2 score (^{99}Tc and ^{129}I) are indeed the most safety-relevant radionuclides. While ^{99}Tc dominates the exposure dose during the first 250,000 years, its comparatively short half-life leads to a flattening of the curve and eventual decline after the peak dose time of 700,000 years has been reached, whereas the dose from ^{129}I keeps rising due to its very slow decay rate, reaching its peak dose after 1.8 million years. As in the case for the horizontal borehole repository in argillite, ^{129}I is by far the most relevant isotope for the long-term safety of the repository, with all the other radionuclides combined contributing less than 1% to the total peak dose.

The three uranium isotopes ^{236}U, ^{238}U, and ^{235}U were also identified as safety-relevant, mainly because of their large inventories and long half-lives. Despite conservatively low sorption coefficients assumed in this study, uranium transport through the geosphere is considerably retarded. As a result, the peak dose has not yet been reached within the performance period of 10 million years. Nevertheless, it is unlikely that these uranium isotopes reach peak dose values that are comparable to or even exceed that of ^{129}I, but they may reach relatively high peak dose values, justifying their selection as safety-relevant radionuclides. The curves shown in blue colors are related to radionuclides that passed the S_1 threshold but failed to meet the S_2 criterion. Their general location near the bottom of the graph is consistent with their overall ranking in Figure 3. Within this category of radionuclides, ^{237}Np, which has a sizeable contribution from ingrowth due to the decay of ^{241}Am, reaches the highest peak dose, followed by the mobile fission products ^{126}Sn and ^{79}Se.

Even though they were screened out as being irrelevant for PA calculations, two radionuclides—^{36}Cl and ^{107}Pd—appear in Figure 6, suggesting that their potential safety-relevance may have been overlooked. While their contributions to peak dose are indeed insignificant (with dose fractions of less than 10^{-4} and 10^{-15}, respectively), the omission of ^{36}Cl, which commands the third highest peak dose, requires an explanation and potential modification of the screening approach. As shown in Figure 3, ^{36}Cl failed to pass the initial screening step, where the inventory is a dominant factor influencing the selection. ^{36}Cl received a comparably low S_1 score because the fast migration of radionuclides through the fracture continuum increased the number of relatively short-lived radionuclides with high specific activities that pass the 10^{-6} threshold value of the normalized S_1 score. For example, ^{239}Pu, ^{240}Pu, ^{229}Th, ^{243}Am, and ^{226}Ra all have high S_1 scores, even though they are excluded in the second screening

step, where the consideration of retardation effects identifies radionuclides with low sorption coefficients and long half-lives as being safety relevant. Both ^{36}Cl and ^{107}Pd have low K_d values and long half-lives, i.e., they are comparatively more mobile and decay more slowly than many of the actinides that ranked higher during the first screening step and prevented ^{36}Cl and ^{107}Pd from making the shortlist. This issue can readily be avoided by either lowering the threshold value or by evaluating all screening factors concurrently rather than in a stepwise approach. In fact, by doing so, ^{36}Cl would pass the more stringent S_2 selection criterion of 10^{-3} and be ranked within the top group of most safety-relevant radionuclides.

In summary, the proposed screening approach correctly identifies the radionuclides with the dominant contribution to the total peak dose even for a repository system located in a fractured host formation, which makes the estimation of peak dose times more intricate. This added complexity results in the conservative inclusion of additional radionuclides, whose dose contributions eventually proved to be irrelevant for this particular case and its representation in the PA model. Conversely, the tiered selection approach may exclude radionuclides in the initial screening step even though they may become more safety-relevant once additional factors are evaluated. These observations lead us to recommend the following minor adjustments to the approach outlined in Section 2.1:

- Select a low threshold value for the first screening step (e.g., 10^{-9}), or examine all radionuclides present in the inventory in a single step, bypassing the evaluation of S_1 (Equation 1) and instead directly using S_2 (Equation 8). Combining the first and second set of factors acknowledges that for deep repository performance assessments, radionuclide transport (specifically retardation effects) can be more important than the factors describing the inventory and source term, which dominate pre-closure safety and some disruptive scenarios (e.g., human intrusion).
- After completing the selection process, replace the individually estimated transport times for radionuclide i, i.e., the term $(R_{Kd_i} \cdot R_{md_i} \cdot t_t)$ in Equation 8, with the transport time of the radionuclide i_{max} with the highest S_2 score, i.e., $(R_{Kd_{imax}} \cdot R_{md_{imax}} \cdot t_t)$, recalculate S_2 and re-rank the resulting scores for a final determination of safety-relevant radionuclides. This second iteration assures that the time available for radioactive decay is the same for all radionuclides and close to the time when the total peak dose is expected to be reached. Note that this refinement invariably leads to lower normalized safety-relevance metrics for all radionuclides, i.e., taking the peak dose without accounting for the time when it occurs is conservative, but may result in a slightly different ranking order (but without affecting the top-ranked radionuclide).
- If considered warranted, refine the estimation of the transport time t_t (Equation 3). For example, (a) instead of assuming that the various repository components are arranged in series, the times could be averaged assuming transport occurs through conduits arranged in parallel or a combination of these two configurations; (b) the assumption that the system for diffusive penetration of the geosphere is linear (Equation 4) could be replaced by equations for cylindrical, spherical, or fractal systems, as appropriate for the actual geometry of the repository layout (specifically length and spacing of the disposal sections); and (c) the advective transport time (Equation 5) could be revised to account for different segments of the transport pathways with potentially different material properties and driving forces.

Refining the screening model naturally involves additional assumptions, computations, and the collection of more data that characterize the repository system and its properties. Whether such extra effort is warranted depends not only on the availability of such data at the current stage of repository development but also on the required accuracy and thus objectives of the subsequent PA modeling study.

4 Concluding remarks

To assess the safety of a geologic repository for the disposal of spent nuclear fuel or high-level radioactive waste, complex numerical models are used to simulate the fate and transport of radionuclides from the breached disposal canisters to the accessible environment, where the radiological exposure dose is calculated as a key metric of repository performance. While the waste form contains a large number of radioisotopes, typically only a small subset thereof materially contributes to the peak dose, depending on the characteristics of the waste form as well as the layout and properties of the engineered and natural barrier systems. We proposed a screening approach that allows for a fast determination of the radionuclides that are likely to be safety-relevant and therefore should be tracked in a high-fidelity performance assessment (PA) model.

To validate the appropriateness and robustness of the approach, an integrated multi-physics model is used to simulate the disposal of SNF assemblies in a deep horizontal and vertical borehole repository, tracking (a) a comprehensive set of radionuclides, and (b) the small subset of radionuclides identified by the screening model as being safety relevant. If the difference in the peak dose values is acceptably small, the screening approach is considered useful and applicable to selecting radionuclides for numerical analyses at various stages of repository development. The following observations and conclusions can be made:

- The proposed screening approach robustly identifies a group of radionuclides that includes those with the highest contribution to peak dose.
- The approach combines factors that are specific to the radionuclide, the repository system, and the model scenario. It can be applied to various waste forms, disposal concepts, and simulation cases (i.e., nominal, disruptive, and accident scenarios).
- The selection criteria of the screening approach can be adjusted to meet the desired level of conservatisms, making sure that the impact of omitted radionuclides on conclusions drawn from the results of a comprehensive PA model is insignificant.
- The approach is based on a comparison of relative rather than the calculation of absolute peak dose values, making the results

less susceptible to uncertainties or systematic errors in the input data; calculating the absolute exposure dose is the task of the high-fidelity PA model.
- The approach can be refined, as warranted, to more accurately capture alternative configurations and secondary processes.
- The approach defensibly reduces the number of radionuclides that need to be tracked in a computationally demanding model, allowing the subsequent modeling studies to focus on safety-relevant issues and the quantification of prediction uncertainties.
- The screening approach was validated for two different disposal systems, each leading to a very different list of safety-relevant radionuclides and corresponding peak exposure doses. This validation exercises provided confidence in both the appropriateness and general applicability of the screening model.

The proposed screening approach is considered applicable to a rather wide range of disposal concepts and analysis scenarios. This assertion is based on the following facets of the approach:

- While highly simplified, the screening model includes key factors representing the waste form, canister performance, repository type and design, geological setting, and prevalent conditions.
- The input parameters of the screening model can be adjusted to mimic the problem-specific characteristics of the PA model, ensuring that the set of safety-relevant radionuclides is tailored to the specific scenario and objectives to be addressed by the PA simulation.
- The outcome of the screening model is a ranking of the radionuclides' *relative* peak-dose contribution rather than estimates of the *absolute* exposure dose. Estimating ranks of relative dose contribution is considerably easier and more robust than determining the absolute exposure dose, which is the responsibility of the high-fidelity PA model.
- The two validation test cases along with additional scenarios summarily discussed in this paper demonstrate that the screening model is capable of generating vastly different lists of safety-relevant radionuclides despite having used a common waste inventory, and that the peak dose calculated by the comprehensive PA model, which tracks many more radionuclides, is indeed dominated by the few radionuclides identified as safety relevant by the simple screening model.

Health impacts from exposure to ionizing radiation change with time and the circumstances of exposure. Consequently, the list of safety-relevant radionuclides is expected to be drastically different if considering an accident at the land surface shortly after fuel removal, or exposure occurring in the distant future by ingestion of groundwater contaminated with radionuclides that leaked from a geologic repository. This large difference in both the risk factors (which include the number of safety-relevant radionuclides), and the consequences is the fundamental reason why geological repositories are the preferred disposal option for radioactive waste. The fact that only a relatively small number of radionuclides tend to dominate the peak exposure dose is an inherent feature of a well-designed and carefully sited repository. The proposed screening approach accounts for the factors controlling repository safety, thus arriving at a defensible, robust, and conservative set of safety-relevant radionuclides tailored to models that support performance assessments at various stages of repository development.

Data availability statement

The original contributions presented in the study are included in the article/supplementary material, further inquiries can be directed to the corresponding author.

Author contributions

SF: Software, Visualization, Writing – original draft, Data curation, Formal Analysis, Methodology, Validation, Conceptualization, Investigation. MH: Writing – review and editing, Data curation. JS: Writing – review and editing, Project administration, Funding acquisition, Supervision.

Funding

The author(s) declared that financial support was received for this work and/or its publication. The information, data, or work presented herein was funded in part by the Advanced Research Projects Agency-Energy (ARPA-E), U.S. Department of Energy, under Award Number DEAR0001621. The views and opinions of authors expressed herein do not necessarily state or reflect those of the United States Government or any agency thereof.

Acknowledgements

The authors greatly appreciate the diligent reviews and constructive comments by S. Norris and C.-P. Jen.

Conflict of interest

Author SF was employed by Finsterle GeoConsulting, LLC.
Author MH was employed by Hannon Clean Energy, LLC.
Author JS was employed by Deep Isolation Nuclear.

Generative AI statement

The author(s) declared that generative AI was not used in the creation of this manuscript.

Any alternative text (alt text) provided alongside figures in this article has been generated by Frontiers with the support of artificial intelligence and reasonable efforts have been made to ensure accuracy, including review by the authors wherever possible. If you identify any issues, please contact us.

Publisher's note

References

Achtziger-Zupančič, P., Loew, S., and Mariéthoz, G. (2017). A new global database to improve predictions of permeability distribution in crystalline rocks at site scale. *J. Geophys. Res. Solid Earth* 122, 3513–3539. doi:10.1002/2017JB014106

Ansolabehere, S., Deutch, J., Driscoll, M., Holdren, J. P., Joskow, P. L., Lester, R. K., et al. (2003). *The future of nuclear power: an interdisciplinary MIT study*. Cambridge, MA, USA: Massachusetts Institute of Technology MIT.

Bates, E. A. (2015). *Optimization of deep boreholes for disposal of high-level nuclear waste*. Cambridge, MA: Doctoral Dissertation, Massachusetts Institute of Technology.

Carbol, P., and Engkvist, I. (1997). *Compilation of radionuclide sorption coefficients for performance assessment*. Stockholm, Sweden: Svensk Kärnbränslehantering AB SKB.

Carter, J. T., Luptak, A. J., Gastelum, J., Stockman, C., and Miller, A. (2012). *Fuel cycle potential waste inventory for disposition*. Report FCR&D-USED-2010-000031 Rev 5. Washington, DC, USA: U.S. Department of Energy, Office of Used Fuel Disposition. 328.

de Marsily, G. (1986). *Quantitative hydrogeology*. Orlando, Florida: Academic Press.

Finsterle, S. (2021). "iTOUGH2-EOS1nT," in *A nonisothermal two-phase flow simulator for water and multiple tracers, user's guide* (Kensington, Calif: Finsterle GeoConsulting). Available online at: https://www.finsterle-geoconsulting.com/s/iTOUGH2-EOS1nT_Users_Guide.pdf (Accessed February 8, 2026).

Finsterle, S., and Lanyon, B. (2022). Pragmatic validation of numerical models used for the assessment of radioactive waste repositories: a perspective. *Energies* 15, 3585. doi:10.3390/en15103585

Finsterle, S., Commer, M., Edmiston, J., Jung, Y., Kowalsky, M. B., Pau, G. S. H., et al. (2017). iTOUGH2: a simulation-optimization framework for analyzing multiphysics subsurface systems. *Comput. & Geosciences* 108, 8–20. doi:10.1016/j.cageo.2016.09.005

Finsterle, S., Muller, R. A., Grimsich, J., Apps, J., and Baltzer, R. (2020). Post-closure safety calculations for the disposal of spent nuclear fuel in a generic horizontal drillhole repository. *Energies* 13, 2599. doi:10.3390/en13102599

Finsterle, S., Cooper, C., Muller, R. A., Grimsich, J., and Apps, J. (2021a). Sealing of a deep horizontal borehole repository for nuclear waste. *Energies* 14 (1), 91. doi:10.3390/en14010091

Finsterle, S., Muller, R. A., Grimsich, J., Bates, E. A., and Midgley, J. (2021b). Post-closure safety analysis of nuclear waste disposal in deep vertical boreholes. *Energies* 14 (19), 6356. doi:10.3390/en14196356

Finsterle, S., McLachlan, J. R., Hannon, M. J., Sloane, J., Abergel, R., and Peterson, P. F. (2025a). Modelling glass degradation and release of radionuclides from vitrified waste for performance assessment simulations. *Front. Nucl. Eng.* 4, 1729916. doi:10.3389/fnuen.2025.1729916

Finsterle, S., Waples, M., Yang, M., and Travis, K. P. (2025b). Generation and dissipation of corrosion gas in a deep horizontal borehole repository for radioactive waste. *Front. Nucl. Eng.* 4, 1689795. doi:10.3389/fnuen.2025.1689795

IAEA (2003). *Reference biospheres for solid radioactive waste disposal, report IAEA-BIOMASS-6*. Vienna, Austria: International Atomic Energy Agency, 560.

ICRP (2012). *Compendium of dose coefficients based on ICRP publication 60*. ICRP publication 119. *Ann. Int. Comm. Radiological Prot.* 41 (Suppl. l.). 130.

Millington, R. J., and Quirk, J. P. (1961). Permeability of porous solids. *Trans. Faraday Soc.* 57, 1200–1207. doi:10.1039/tf9615701200

Muller, R. A., Finsterle, S., Grimsich, J., Baltzer, R., Muller, E. A., Rector, J. W., et al. (2019). Disposal of high-level nuclear waste in deep horizontal drillholes. *Energies* 12, 2052. doi:10.3390/en12112052

Nagra (1994). "Kristallin-I: safety assessment report," Nagra Technical Report NTB 93-22 (Wettingen, Switzerland: National Cooperative for the Disposal of Radioactive Waste (Nagra)). 468.

Nagra (2002). "Models, codes and data for safety assessment," in *Nagra Technical Report NTB 02-06* (Wettingen, Switzerland: National Cooperative for the Disposal of Radioactive Waste (Nagra). 504.

Nagra (2024). "Safety assessment methodology," Nagra Technical Report NTB 24-19. Wettingen, Switzerland: National Cooperative for the Disposal of Radioactive Waste (Nagra). 102.

Neretnieks, I. (1980). Diffusion in the rock matrix: an important factor in radionuclide retardation? *J. Geophys. Res.* 85 (B8), 4379–4397. doi:10.1029/jb085ib08p04379

Pruess, K., Oldenburg, C., and Moridis, G. (2012). *TOUGH2 User's guide, version 2.1*. Berkeley, Calif: Lawrence Berkeley National Laboratory.

SNL (2013). *Generic deep disposal safety case*. Albuquerque, New Mexico: Sandia National Laboratories.